iSprawl: Design and Tuning for High-speed Autonomous Open-loop Running

Sangbae Kim
Center for Design Research
Stanford University
Stanford, CA 94305-2232, USA
sangbae@stanford.edu

Jonathan E. Clark
GRASP Laboratory
University of Pennsylvania
Philadelphia, PA 19104, USA
jonclark@grasp.upenn.edu

Mark R. Cutkosky
Center for Design Research
Stanford University
Stanford, CA 94305-2232, USA
cutkosky@stanford.edu

Abstract

We describe the design features that underlie the operation of iSprawl, *a small (0.3 kg) autonomous, bio-inspired hexapod that runs at 15 body-lengths/second (2.3 m/s). These features include a tuned set of leg compliances for efficient running and a light and flexible power transmission system. This transmission system permits high speed rotary power to be converted to periodic thrusting and distributed to the tips of the rapidly swinging legs. The specific resistance of* iSprawl *is approximately constant at 1.75 for speeds between 1.25 m/s and 2.5 m/s. Examination of the trajectory of the center of mass and the ground reaction forces for* iSprawl *show that it achieves a stable, bouncing locomotion similar to that seen in insects and in previous (slower) bio-inspired robots, but with an unusually high stride frequency for its size.*

KEY WORDS—biorobotics, legged locomotion, hexapod, compliance

1. Introduction

In recent years a number of robots have been developed that draw their inspiration from running arthropods or insects including *Sprawlita* (Cham, 2002), *Scorpion* (Klaassen et al., 2002), *Whegs* (Quinn et al., 2003), *Mini-Whegs* (Morrey et al. 2003) and *RHex* (Saranli et al. 2001). When insects are moving rapidly they typically employ an alternating tripod gait and rely heavily on passive mechanical properties to achieve dynamic stability. The sprawled posture with large forces in the horizontal plane, and the compliance and damping in the limbs and joints, serve as "preflexes" (Loeb et al., 1999) that promote stable running and rapid recovery from perturbations (Kubow and Full, 1999; Meijer and Full, 1999).

In the case of the *Sprawl* family of robots, the main principles adapted from insects, the cockroach in particular, are:

- a bouncing, alternating tripod gait based on a substantially feed-forward motor pattern (Full et al., 1998)
- limb specialization in which the rear legs primarily accelerate the body while the front legs decelerate it (Full et al., 1991)
- legs that generate ground reaction forces directed from the feet through the hips (Full et al., 1991)
- "hip" joints with significant passive rotational stiffness and damping that help stabilize the gait and recirculate the legs during the swing phase (Garcia et al., 2000; Meijer et al., 2000; Kubow and Full, 1999)

The *Sprawl* robots are fabricated using a multi-material rapid prototyping process, Shape Deposition Manufacturing (Cham, 2002; Weiss et al., 1997), that makes it possible to achieve local variations in structural compliance and damping and to embed components such as sensors and actuators

The International Journal of Robotics Research
Vol. 25, No. 9, September 2006, pp. 903-912
DOI: 10.1177/0278364906069150

Figures appear in color online: http://ijr.sagepub.com

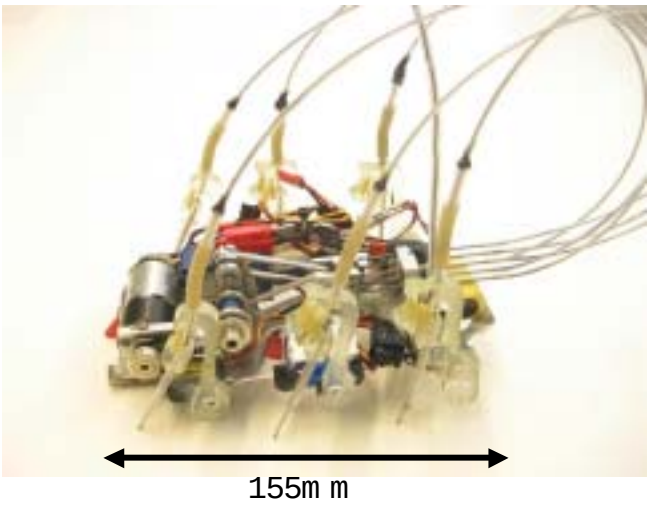

Fig. 1. *iSprawl*: a fully autonomous hexapedal robot driven by an electric motor and flexible push-pull cables.

for increased ruggedness. Like their exemplars, the *Sprawl* robots are capable of fast locomotion over rough terrain and of executing rapid turns by changing leg thrust angles (McClung et al., 2004).

The robots can run without any proprioceptive or exteroceptive feedback; however, the addition of ground contact sensors allows the stride period to adapt automatically to changes in terrain or slope (Cham et al., 2001) and the addition of antennae allows the robots to follow walls at running speeds (Cowan et al., 2005). A closer look at the dynamics of the running robots reveals motions and ground reaction forces similar to those found in insects and other small animals. This locomotion pattern has been termed SLIP (spring loaded inverted pendulum) in the literature and is seen in many running animals (Full and Koditschek, 1999).

A limiting factor in the design of previous *Sprawl* robots has been their use of pneumatic pistons for propulsion. Although electric motors are ubiquitous in small robots, pistons were chosen for the *Sprawl* robots as powerful, compact linear actuators. The main disadvantage of pneumatic pistons is that they virtually preclude autonomous operation. The volume of compressed gas needed for 10 minutes of operation is such that a gas storage tank would be too heavy to carry on board. Clearly this is a problem since for practical application, legged robots need to be power autonomous.

In this paper, we present an independent version of the *Sprawl* robots utilizing electric propulsion. The incorporation of a new power transmission system, lithium polymer batteries, and a redesigned set of compliant legs have enabled *iSprawl* to run autonomously at speeds of over 15 body-lengths/second (2.3 m/s). Despite significant changes in the actuation and force generation mechanism, we show that by appropriately tuning the passive compliance in the legs the fast, self-stabilizing behavior of the robot is preserved. This invariance to actuation scheme underscores the generality of the locomotion principles encapsulated in the *Sprawl* family of robots.

2. Mechanical Design of *iSprawl*

The most challenging aspects of utilizing electrical actuation for the *Sprawl* robots are converting continuous rotation to periodic thrusting and incorporating sufficient flexibility into the power train to accommodate the repositioning of the legs. Several schemes were investigated before settling on the system presented in this paper.

One major concern is power density, for which it is desirable to use a single high-speed electric motor as the primary actuation source. For large robots, the actuator energy can be stored elastically and periodically released, as in the case of the Bow Legged Hopper (Brown and Zeglin, 1998) and a number of subsequent legged robots (Nichol and Waldron, 2002). At the scale of *iSprawl* however, it becomes easier to store kinetic energy. This is the approach shown in Figure 2, in which a rotating double crank-slider mechanism stores rotational kinetic energy and converts it to alternating push–pull motions for each tripod of legs. As discussed in the Appendix, the total rotational kinetic energy is approximately equal to the power consumed per stride while running.

The push–pull actions must also be distributed to the tips of the flexible, swinging legs. One possible solution is to employ liquid using a master/slave piston arrangement and flexible tubes. An early variant named "Aquasprawl" employed this method and achieved speeds of 3 body-lengths/second. A lighter and more efficient alternative is to use flexible cables in low-friction sleeves, as shown in Figure 3. By adding rigid elements to both ends of the shaft and tube, the cables are able to thrust as well as pull. The end result is that the legs of *iSprawl* have a very low rotational inertia and a passive swing frequency of 45 Hz.

As in previous *Sprawl* robots, the motions of the legs back and forth with each step are achieved passively by operating the robot as a resonant system. During each stance phase the hip springs (flexures) are loaded by the motion of the body. During the swing phase this stored energy is used to reposition the legs to their nominal orientation. In addition, remote control servos are mounted at the hips of the middle legs to change the equilibrium leg angles to effect turns, as motivated by the results of McClung et al. (2004). The physical specifications for *iSprawl* are given in Table 1.

3. Tuning Parameters for Smooth Open-loop Running

When first assembled, *iSprawl* achieved speeds of approximately 5 body-lengths/second. Review of high-speed video

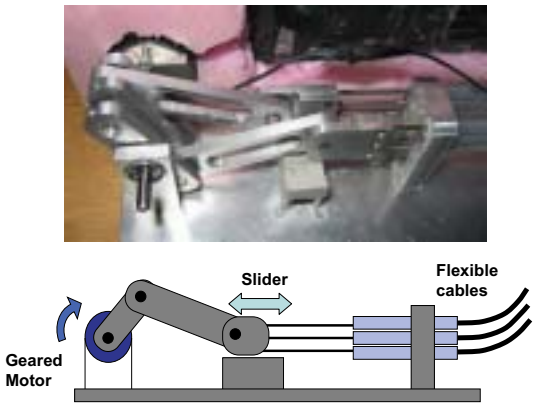

Fig. 2. Power transmission system for *iSprawl*. A double crank-slider is used to store and convert the rotational energy from the motor to linear oscillations.

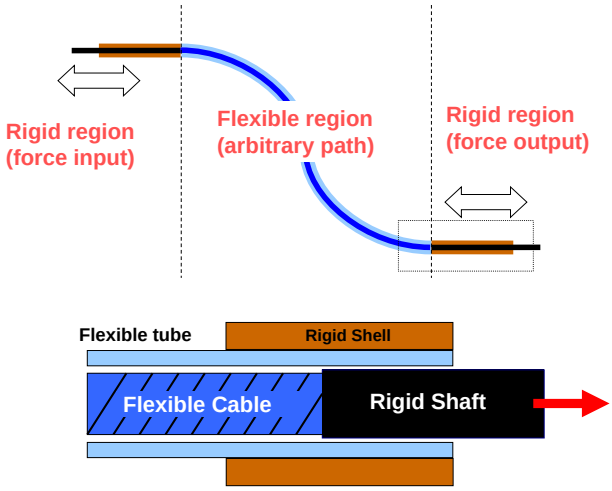

Fig. 3. Power transmission system for *iSprawl*. Schematic sketch shows the flexible and rigid sections of the push–pull cables.

of its motion on a treadmill revealed numerous sources of inefficiency, including excessive and irregular pitch and roll oscillations and bouncing and slippage of the feet. These effects were gradually reduced by adjusting the center of mass location and the equilibrium angles of the front, middle and rear legs following a procedure similar to that of Clark (2004). At this point it became clear that foot contact forces were increasing too rapidly after initial contact, causing abrupt changes to

Table 1. Physical Parameters for *iSprawl*

Body size	155 × 116 × 70 mm (excluding cables)
Body mass	0.3 kg (including batteries and servo circuit)
Maximum speed	2.3 m/s (15 bodylength/s)
Stride frequency	14 Hz
Power consumption	12 W
Motor	Maxon A-max series, 6Watt; 22 mm dia. Rated voltage : 6V (actual = 22V) Rated torque : 7.36mNm at 6V Rated current : 756 mA at 6V Actual speed : 21384 rpm at 22V
Gear head	19.8:1, Maxon ϕ24 spur gear
Timing belt	3.2 mm wide, 9:7 speed ratio
Legs	Polyurethane 72DC and 90A from Innovative Polymers Inc.
Servo motors	Hitech H5-55 (1.3 Kg cm)
Typical leg motion	25 mm stroke, 25° swing
Battery	6 pack lithium polymer (3.7 × 6 V, 250 mAh per pack)
Battery life	approx. 5 min. at running speed

the momentum of the robot and reducing efficiency. The effect is not surprising given that we have replaced a compliant force actuator (pneumatics) with a fixed displacement actuation from the slider-crank mechanism. To achieve a smoother, more SLIP-like motion, it was necessary to add tuned axial compliance to the push/pull cables, as shown in Figure 4.

3.1. Desired Leg Extension Profile

The hypothesis used in tuning the axial leg compliances is that the ideal motion of the robot is a smooth low-amplitude oscillation in the vertical plane and a nearly constant forward velocity, as indicated in Figure 5. The constants used in these calculations are listed in Table 2.

Table 2. Parameters for Single Analytic Leg Model in Figure 5

θ_i	70°	Leg initial angle
θ_f	45°	Leg final angle
f	14 Hz	Leg oscillation frequency
v	2.3 m/s	Body forward velocity
h_{nom}	35 mm	Nominal body height
Δh	1 mm	Change in body height

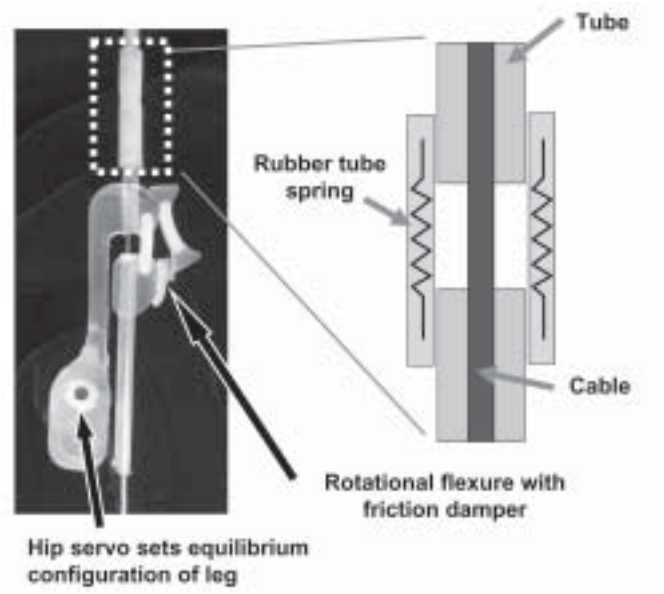

Fig. 4. Schematic of the leg compression spring design utilizing a tension spring in the flexible tubing around the push–pull cable. Also shown are the frictional dampers (on front and middle legs).

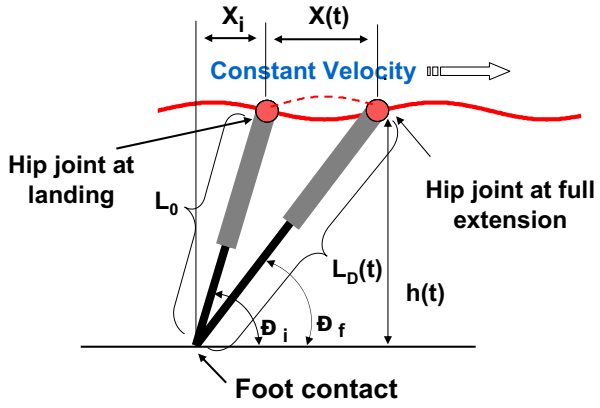

Fig. 5. Schematic of the desired leg extension profile needed to produce a sinusoidal trajectory of the center of mass during stance. Dashed line shows trajectory that would occur without compression.

We begin by assuming that the height, h, of the body follows a sinusoidal path:

$$h(t) = h_{nom} + \Delta h \, sin(2\pi \; 2f \; t) \tag{1}$$

where h_{nom} is the nominal body height, Δh is amplitude of oscillation, and $2f$ is the body oscillation frequency (the body's vertical oscillation frequency is twice the leg actuation frequency). The initial leg length, L_0, is given by:

$$L_0 = h_{nom}/sin(\theta_i) \tag{2}$$

where θ_i is the leg angle at touchdown. The horizontal position of the body at touchdown is given by:

$$X_i = L_0 cos(\theta_i) \tag{3}$$

and the forward position as a function of time is given by:

$$X(t) = v \; t \tag{4}$$

which assumes a constant horizontal velocity, v. (This is a reasonable assumption as the actual forward speed varies by less than 3% over a stride.)

For the leg to remain in contact, the desired leg length, $L_D(t)$, is given by:

$$L_D(t) = \sqrt{h(t)^2 + (x_i + x(t))^2}. \tag{5}$$

For *iSprawl* the nominal leg extension trajectory, $L_{nom}(t)$, which is a function of the crank-slider mechanism (see Appendix for details) can be approximated as:

$$L_{nom}(t) = A_0 \; sin(2\pi f t) + L_0 \tag{6}$$

where $A_0 = 12.7$ mm. The leg compression, L_s, is given by:

$$L_s(t) = L_0 + L_{nom}(t) - L_D(t). \tag{7}$$

The solution of these equations yields the maximum leg spring compression during stance $\Delta L = \max(L_s(t)) = 4$ mm.

The body oscillates vertically at a frequency of $2f = 28$ Hz, leading to a peak vertical acceleration of:

$$\ddot{h}_{max} = \Delta h (2\pi \; 2f)^2 \tag{8}$$

and a maximum vertical ground reaction force of:

$$F_{h,max} = mg + m\Delta h (4\pi f)^2 \tag{9}$$

With a body mass, m, of 0.31 kg the maximum predicted force, $F_{h,max}$, is 12.2 N, which correlates well with the peak measured ground reaction forces found in Section 3.4. The peak force occurs at a leg angle, θ, of approximately 55°, about half way through stance. Although the leg is not a free pin joint due to rotational hip compliance, we assume that the force is acting primarily along the axis of the leg.

Thus the effective whole body leg spring constant should be:

$$k = \frac{12.2\,\text{N}/\sin(55^\circ)}{4\,\text{mm}} = 3.7\,\text{N/mm}. \tag{10}$$

The front legs have the largest contribution (roughly 50%) to the vertical stiffness of the tripod. Accordingly, springs

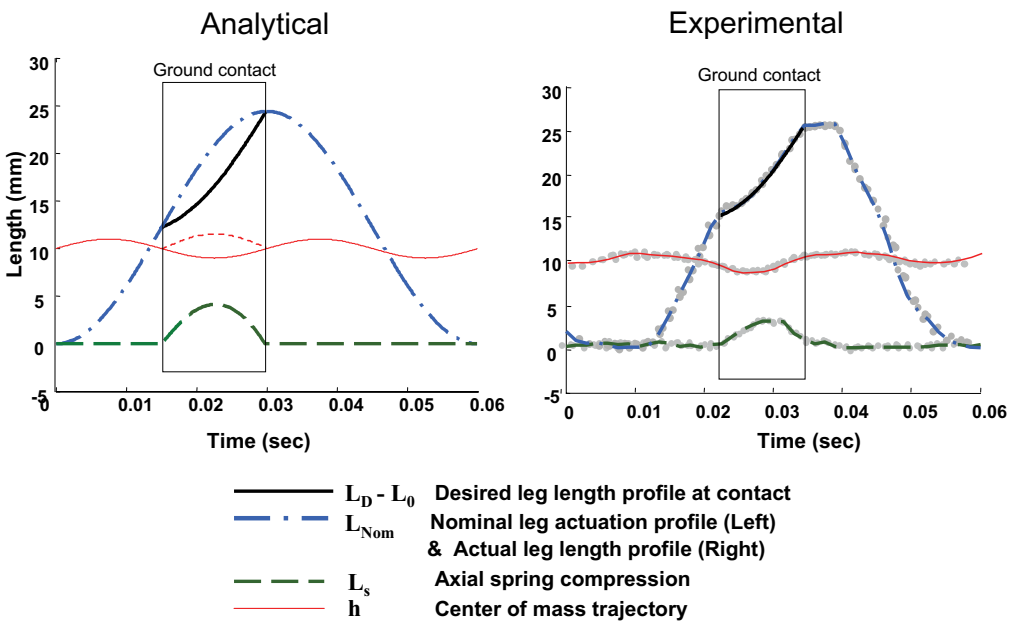

Fig. 6. The theoretical and experimental leg extension profiles for *iSprawl* running at 2.3 m/s. Also shown are the path of the COM and the extension of the axial spring for each case. The dashed line in the analytical plot shows the COM trajectory that would occur without any spring compression. Curves for the measured leg extension and COM trajectory represent averages of three successive strides shown in gray dots.

with a stiffness of 1.7 N/mm inserted into the legs were found to give best performance. Note that to achieve the effect of a compression spring in series with the push–pull cables, it was actually easier to insert a corresponding tension element (a short section of latex rubber tubing) into the otherwise inextensible sheaths (Figure 4).

Figure 6 shows the theoretical and the measured leg and body trajectories for a single stride. The trajectories for the measured case were obtained by filming *iSprawl* at 500 frames/second as it ran on a treadmill. The estimated positional accuracy is ± 0.1 mm. The dark lines represent the desired leg extension profile during contact, and the thin lines represent the trajectory of the center of mass. The dashed segment of this line in the analytical plot indicates the center of mass trajectory that would occur without the leg spring, whose compression is indicated by the dashed line at the bottom of the plot. The experimental data show that both the leg extension and center of mass trajectories match the model predictions closely. The experimentally measured axial spring compression is slightly smaller than the predicted value. This is compensated for by the inherent elasticity of the push–pull cable system. We note that the actual ground contact is slightly delayed with respect to the predicted value due to some backlash in the transmission system.

Adding axial compliance to the legs increased the robot's speed by 50%. It also reduced mechanical failures and produced a smoother period-1 gait.

In addition to tuning the axial compliance of the leg extension system, it was necessary to adjust the rotational compliance and damping of the passive hips. As with the earlier *iSprawl* robots, the legs are multi-material structures of hard and soft urethane. If the urethane flexures are too stiff, the legs do not flex enough and the stride length is reduced; if they are too soft the robot stumbles and loses open-loop stability (Clark, 2004). Empirically, rotational stiffnesses of approximately 72 Nmm for the front legs, 54 Nmm for the middle, and 36 Nmm for the rear legs were found to give best results. In earlier *Sprawl* robots, the inherent visco-elasticity of the soft urethane provided adequate damping; for *iSprawl* it was necessary to add small friction dampers to the front and middle legs, as can be seen in Figure 4.

3.2. Performance

Figure 7 shows the relationship between the robot's forward velocity and its stride period. The normal operating point for the robot is at 14–15 Hz, which corresponds to a speed of about 2.3 m/s. The relationship between forward speed and actuation frequency is nearly linear above 4 Hz, with no perceptible change in the motion pattern.

Another value that has been used to measure locomotion speed in a scale-independent manner is the Froude number, F,

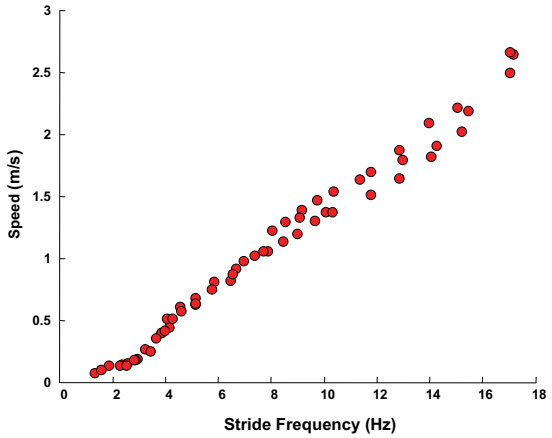

Fig. 7. Running speed of *iSprawl* vs. stride frequency

a dimensionless value that relates the inertial force to gravitational force or alternatively the translational kinetic energy to the gravitational potential energy of the system. The Froude number is typically defined as:

$$F = \frac{v}{\sqrt{gl}}$$

where v is the velocity of locomotion, g is the gravitational constant, and l is a characteristic leg length, often taken in running robots as the distance from the hip to the ground. It should be noted that occasionally the Froude number is expressed as the square of how we have defined it. Alexander and Jayes (1983) have shown that a wide variety of animals transition from a walk to a trot and a trot to a gallop at similar Froude numbers. *iSprawl* exhibits a gait transition from walking to running (as defined by the phasing of its kinetic and gravitational potential energy) at about 3.5 Hz (F = 0.6), which is close to the $F = 0.7$ value preferred by most animals (Kram et al., 1997b). When running at its nominal frequency of 14 Hz *iSprawl's* Froude number is about 1.9.

iSprawl's top speed of 2.3 m/s is about 15% slower than the current fastest autonomous hexapedal runner *RHex*, but as *iSprawl* is only about 1/3 as long, its speed relative to size (body-lengths/second) is much larger. The performance of *iSprawl* is the same whether running on a treadmill or on paved surfaces. It easily traverses obstacles less than 2 cm high. In soft terrain, the robot becomes mired due to its small feet. Perhaps a better comparison would be to *Mini-Whegs* (Morrey et al., 2003), which at 0.09 m long and 0.150 kg is a little more than half the size of *iSprawl*. *Mini-Whegs* uses rimless "wheel-legs" as its appendages, which enables it to climb over relatively larger obstacles, but it runs at a slower relative speed. In addition the thrusting legs of *iSprawl* allow it to make more rapid turns (turn radius of 1.5 vs. 2.5 body-lengths for *Mini-Whegs*) at speeds below 1 m/s.

3.3. Energetics

Since the power supply contributes a relatively significant portion of total mass, energy efficiency is of crucial importance for autonomous legged robots. With the switch from a pneumatic to an electro-mechanical actuation scheme, a significant energetic improvement is realized. Furthermore the precise measurement of the total power consumption is straightforward.

Figure 8 shows the total power consumption while running on a treadmill and the non-productive power consumption (i.e., while running in air) as a function of stride frequency. The latter data set should be taken as a lower bound because the transmission forces, and the corresponding friction forces, are higher when the robot is in contact with the ground.

When driven at low frequencies *iSprawl's* power consumption has a larger relative variation since the required motor torque fluctuates throughout stride. Beyond 5 Hz, the robot runs with a stable gait and a constant power consumption which is linearly proportional to stride frequency. At its top speed *iSprawl* has enough battery life to run continuously for about 5 minutes.

For comparison with other legged robots, Figure 9 shows the specific resistance, $P(v)/mgv$, as a function of speed, where m is the mass of the robot, v is the forward velocity and $P(v)$ is the total electrical power consumption. For the preferred running speeds of *iSprawl*, corresponding to stride frequencies above 7 Hz and speeds above 1 m/s, the specific resistance is nearly constant at 1.75. This value is comparable with that of other running robots, although higher than the most efficient of them (Poulakakis and Buehler, 2005; Weingarten et al, 2004). Looking again at Figure 8, we observe that half the total power is consumed in the motor and transmission system, which suggests that specific resistance could be improved with with a more efficient motor and gearbox and with an effort to reduce the sliding friction in the cables.

3.4. Ground Reaction Forces

A final subject of comparison among *iSprawl*, the earlier *Sprawl* robots, and insects is the pattern of ground reaction forces (GRF). The pattern seen in insects is that the front legs provide a braking force at the start of each step while the rear legs provide most of the forward propulsion at the end of each step (taking touchdown as the beginning of the step). The middle legs provide a mixture of propulsion and braking (Full et al., 1991). In addition, the front legs, being most nearly upright, have the largest vertical and smallest horizontal forces. The top two rows of Figure 10 show the averaged GRFs for a cockroach running and for *Sprawlita*, one of the

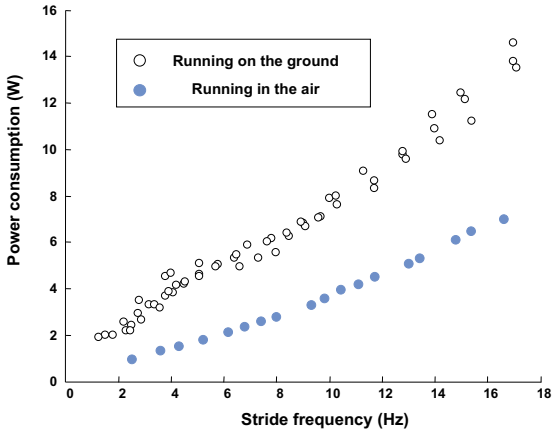

Fig. 8. Electrical power consumption of *iSprawl* without load and with running load.

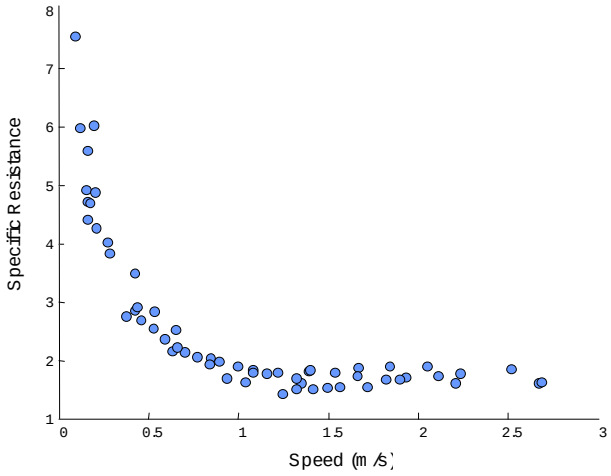

Fig. 9. Specific resistance vs. speed for *iSprawl* running on smooth terrain.

first *Sprawl* robots with pneumatic pistons (from Cham et al. 2002). These patterns are similar except that the rear legs of the robot produce a negative horizontal force (drag) at the end of each stride rather than at the beginning as with the insect. The data for *iSprawl* were taken with the robot running at 2.3 m/s over an ATI Omega force plate, and the signal was conditioned in the same manner as in Cham (2002). The resolution of the sensor is at least 1/40 N in the vertical, and 1/80 N in the ground plane. The force pattern for *iSprawl* is similar to *Sprawlita*, with a couple of noticeable differences: the front legs provide less braking force and the rear legs have less drag. The reduction in parasitic foot drag is partly responsible for the greater speed of *iSprawl*. While the net drag of the feet is considerably less than in previous *Sprawl* robots, the tail of the robot still makes intermittent contact with the ground. The non-zero integral of the leg horizontal forces in *iSprawl* is mainly due to this drag force.

4. Discussion of Results and Conclusions

The development of a light and flexible power distribution system has allowed the creation of an autonomous, biologically inspired hexapedal runner. A comparison of the locomotion dynamics of the electrically powered *iSprawl* and the pneumatically driven *Sprawl* robots shows that despite the difference in actuation schemes, both robots demonstrate comparably fast and stable running with an open-loop actuation pattern. This suggests that the key design principles embodied in the *Sprawl* robots (namely: sprawled for–aft posture, thrusting legs, and passive hip joints with rotational compliance and damping) may have practical utility beyond this family of robots. A comparison of the leg extension profiles and ground reaction forces between the electric and pneumatic variants of the *Sprawl* robots shows that despite small differences, the essential motions and forces for fast and stable locomotion have been preserved.

We also found that when the passive properties of the robot, including the center-of-mass location, leg equilibrium angles, and leg stiffnesses were adjusted empirically for smoother running, the robot was able to run more than twice as fast. A more detailed tuning of the leg impedance may result in even faster and more stable running.

In comparison to other legged robots, *iSprawl* achieves an exceptionally high speed and Froude number, chiefly by virtue of having an extremely high stride frequency for its size. A comparison with running animals is somewhat more complicated. *iSprawl's* Froude number of 3.5 is one at which most animals would have switched from a trot to a gallop. There are some notable exceptions such as elephants, which "Groucho-run" with Froude numbers as high as 3.4 (Hutchinson et al, 2003) and cockroaches, which continue to use an alternating tripod gait for Froude numbers as high as 6–7 (Full and Tu, 2000). However, like other animals, cockroaches do not achieve their highest speeds by continuing to increase stride frequencies beyond the normal rate used for running (Full and Tu, 2000). Rather they increase their effective stride length via aerial phases. In contrast, *iSprawl* runs with a stride frequency comparable to that of a mouse although it has a body weight comparable to that of a well fed rat (Heglund et al., 1974). In comparison to other robots and to animals, *iSprawl* is capable of high stride frequencies chiefly because of the very low rotational inertia of its legs. This, in turn, is a direct consequence of having a single actuation source mounted in the

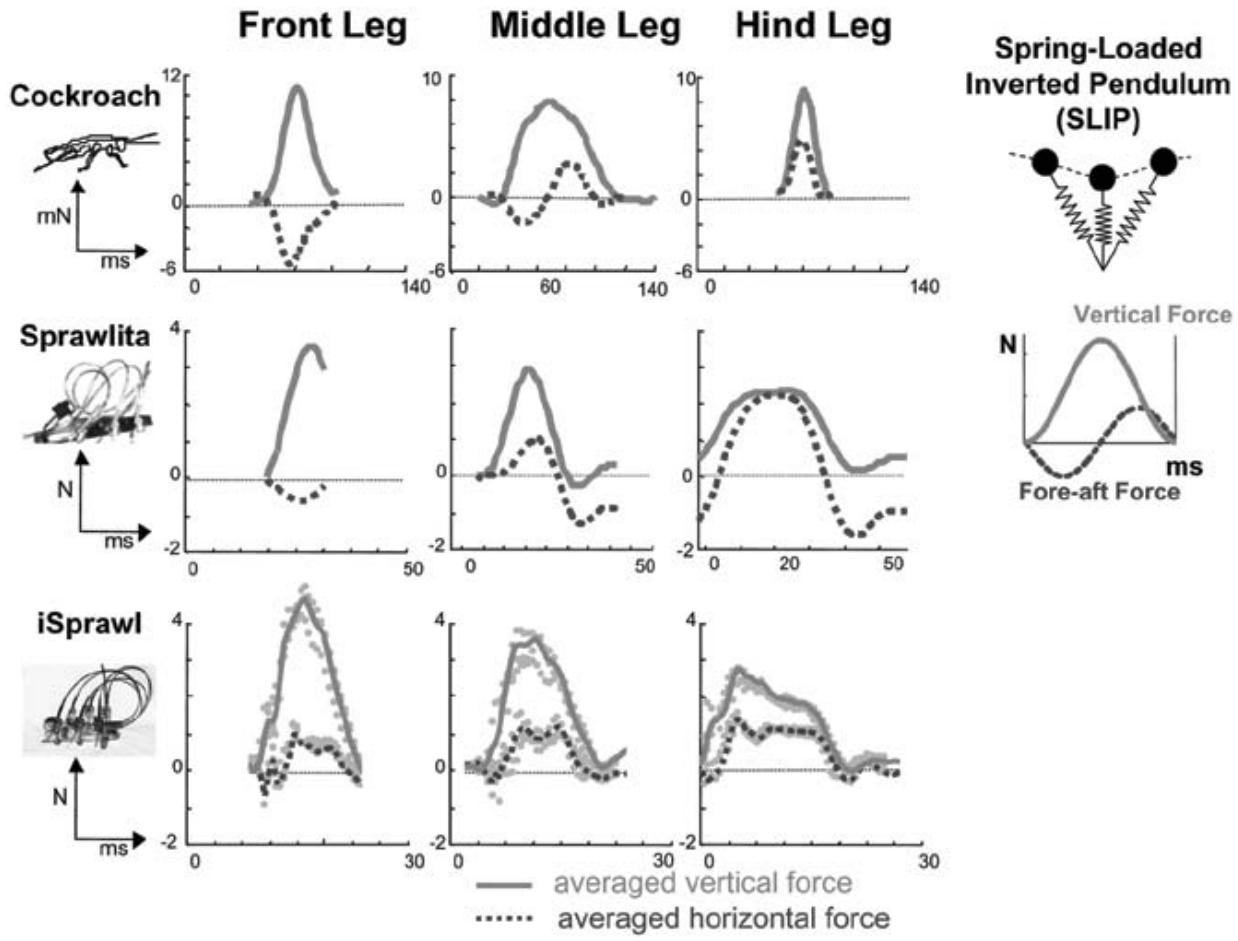

Fig. 10. Vertical and horizontal individual leg ground reaction forces for a cockroach and *Sprawlita* (Cham et al., 2001) and for *iSprawl*, in comparison to the idealized SLIP model (Full and Tu, 2000).

body, with reciprocating motion directed to the feet via push–pull cables. Indeed, given the passive 45 Hz swing frequency of the legs, the maximum running frequency could, in theory, be even higher if a different motor and battery source were used.

Appendix

Crank–Slider Kinematics (see Figure 11)

By inspection, the slider–crank equation is

$$X(t) = a\cos(\omega t) + b\cos(\arcsin(\frac{a}{b}\sin(\omega t)))$$

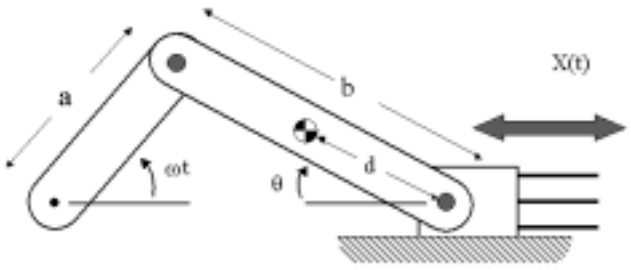

Fig. 11. Schematic of crank and slider

where

$$\omega = 94 \text{ rad/s}$$
$$a = 12.7 \text{ mm}$$
$$b = 38 \text{ mm}$$
$$d = 20 \text{ mm}$$

For these values, the stroke is an approximately sinusoidal motion of amplitude 12.7 mm.

The kinetic energy stored in the double crank and slider mechanism can be calculated from the physical parameters:

$$I_a = 1177.4 \text{ g mm}^2 \text{ (for both cranks)}$$
$$I_b = 2908 \text{ g mm}^2 \text{ (each connecting rod)}$$
$$m_b = 4.32 \text{ g (each connecting rod)}$$
$$m_{slider} = 6.48 \text{ g.}$$

However, the total rotational kinetic energy is dominated by the motor inertia, $I_m = 409$ g mm^2, at $\omega_m = 2239$ rad/second:

$$E_{kinetic} \approx \frac{1}{2} I_m {\omega_m}^2 = 1 \text{ Joule}$$

or about equal to the energy consumed per stride.

Appendix: Index to Multimedia Extensions

The multimedia extension page is found at http://www.ijrr.org.

Table of Multimedia Extensions

Extension	Type	Description
1	Video	Video showing iSprawl running outdoors under remote control (http://bdml.stanford.edu/twiki/pub/Main/IndependentSprawl/iSprawlRC.mov)
2	Video	High-speed video of iSprawl on a treadmill (http://bdml.stanford.edu/twiki/pub/Main/IndependentSprawl/iSprawlSlowMotion.mov)

Acknowledgments

We thank Trey McClung and Emily Ma for their help in conducting the experiments described in this paper and the reviewers for their comments and suggestions on the first draft. The development of the *Sprawl* robots was supported by the Office of Naval Research under grant N00014-98-1-066. Jonathan Clark is supported by the IC Postdoctoral Fellow Program under grant number HM158204-1-2030.

References

Alexander, R. McN. and Jayes, A. S. 1983. A dynamic similarity hypothesis for the gaits of quadrupdeal mammals. *Journal of Zoology* 201:135–152.

Brown, B. and Zeglin, G. 1998. The bow legged hopping robot. *Proceedings of the IEEE International Conference on Robotics and Automation*.

Cham, J. G., Bailey, S. A., Clark, J. E., Full, R. J., and Cutkosky, M. R. 2002. Fast and robust: hexapedal robots via shape deposition manufacturing. *International Journal of Robotics Research* 21(10):869–882.

Cham, J. G., Karpick, J., Clark, J. E., and Cutkosky, M. R. 2001. Stride period adaptation for a biomimetic running hexapod. *International Symposium of Robotics Research*, Lorne, Victoria, Australia.

Clark, J. E. 2004. *Design, Simulation, and Stability of a Hexapedal Running Robot.* PhD thesis, Stanford University.

Cowan, N., Ma, E. J., Cutkosky, M. R., and Full, R.J. 2005. A biologically inspired passive antenna for steering control of a running robot. *Eleventh International Symposium on Robotics Research*, Sienna, Italy, October. Springer Tracts in Advanced Robotics, Vol. 15 (eds P. Dario and R. Chatila).

Full, R. J., Blickhan, R., and Ting, L. H. 1991. Leg design in hexapedal runners. *Journal of Experimental Biology* 158:369–390.

Full, R. J. and Koditschek, D. E. 1999. Templates and anchors: neuromechanical hypotheses of legged locomotion on land. *Journal of Experimental Biology* 202(23):3325–3332.

Full, R. J. and Tu, M. S. 2000. Mechanics of six-legged runners. *Journal of Experimental Biology* 148:129–146.

Full, R. J., Stokes, D. R., Ahn, A. N., and Josephson, R. K. 1998. Energy absorption during running by leg muscles in a cockroach. *Journal of Experimenatal Biology* 201(7):997-1012.

Garcia, M., Kuo, A. D., Peattie, A. M., Wang, P. C., and Full, R. J. 2000. Damping and size: insights and biological inspiration. *International Symposium on Adaptive Motion of Animals and Machines*, Montreal, Canada.

Heglund, N. C., Taylor, C. R., and McMahon, T. 1974. Scaling stride frequencies to animal size: mice to horses. *Science* 186(4169):1112–1113.

Hutchinson, J. R., Famini, D., Lair, D., and Kram, R. 2003. Are fast-moving elephants really running? *Nature* 422:493–494.

Klaassen, B., Linnemann, R., Spenneberg, D., and Kirchner, F. 2002. Biomimetic walking robot SCORPION: Control and modeling. *Proceedings of the ASME Design Engineering Technical Conference*, Vol. 5, pp. 1105–1112.

Kram, R., Domingo, A., and Ferris, D. P. 1997. Effect of reduced gravity on the preferred walk–run transition speed. *The Journal of Experimental Biology* 200:821–826.

Kubow, T. M. and Full, R. J. 1999. The role of the mechanical system in control: a hypothesis of self-stabilization in hexapedal runners. *Philosophical Transactions of the Royal Society of London, Series B-Biological Sciences* 354(1385):849–861.

Loeb, G. E., Brown, I. E., and Cheng, E. J. 1999. A hierarchiacal foundation for models of sensorimotor control. *Experimental Brain Research* 126:1-18.

McClung, A. J., Cham, J. G., and Cutkosky, M. R. 2004. Dynamic maneuvering of a biologically inspired hexapedal robot. *ASME IMECE-61150 Proceedings* (Submitted).

Meijer, K. and Full, R. J. 1999. Stabilizing properties of invertebrate skeletal muscle. *American Zoologist* 39.

Meijer, K., Libby, T. M., and Full, R.J. 2000. Passive stability provided by the musculo-skeletal properties of an insect leg. *American Zoologist* 40(6):1129–1130.

Morrey, J. M., Lambrecht, B., Horchler, A. D., Ritzmann, R. E., and Quinn, R. D. 2003. Highly mobile and robust small quadruped robots. *International Conference on Intelligent Robots and Systems (IROS2003)*, Las Vegas.

Nichol, J. G. and Waldron, K.J. 2002. Biomimetic leg design for untethered quadruped gallop. *Proceedings of the 5th International Conference on Climbing and Walking Robots*, Paris, pp. 49-54.

Poulakakis, I. and Buehler, M. 2005. Modeling and experiments of untethered quadrupedal running with a bounding gait: the Scout II robot. *International Journal of Robotics Research* 24(4):239–256.

Quinn, R. D., Nelson, G. M., Bachmann, R. J., Kingsley, D. A., Offi, J. T., Allen, T. J., and Ritzmann, R. E. 2003. Parallel complementary strategies for implementing biological principles into mobile robots. *International Journal of Robotics Research* 22(3/4):169–186.

Saranli, U., Buehler, M., and Koditschek, D. E. 2001. RHex: a simple and highly mobile hexapod robot. *International Journal of Robotics Research* 20(7):616–631).

Weingarten, J. D., Lopes, G. A., Buehler, M., Groff, R. E., and Koditschek, D.E. 2004. Automated gait adaptation for legged robots. *International Conference in Robotics and Automation*, New Orleans, IEEE.

Weiss, L. E., Merz, R., Prinz, F. B., Neplotnik, G., Padmanabhan, P., Schultz, L., and Ramaswami, K. 1997. Shape deposition manufacturing of heterogenous structures. *Journal of Manufacturing Systems* 16(4):239–248.